

High-temperature gold metallization for ZnO nanowire device on a SiC substrate

Ron Gurwitz, Guy Tuboul, Boaz Shikler, and Ilan Shalish^{a)}

Department of Electrical Engineering, Ben Gurion University of the Negev, Beer Sheva, Israel

(Received 25 April 2012; accepted 17 May 2012; published online 19 June 2012)

Gold is commonly used nowadays in metal contacts to nanowire devices. Due to their small size, nanowire devices often get heat up enough to cause a reaction of the contact and substrate, whether during operation or as a result of a spontaneous pulse of an electrostatic discharge. In most cases, the point of failure is the metallization, as is the case studied here. Gold is useful not only for its good electrical conductance but also because it is a good heat conductor and inert to the ambient. To improve the survivability of a gold metallization for nanowire devices incorporating ZnO nanowire atop a SiC substrate, we used a sputter-deposited Ti-Si-N ternary diffusion barrier layer and a Ti adhesion layer between the top gold layer and a 4H-SiC substrate that survives 30 min of vacuum annealing at 850 °C and 5 days of annealing at 500 °C in Ar. Rutherford backscattering spectrometry and x-ray photoelectron spectroscopy were used to test the integrity of the layers before and after annealing both with and without the diffusion barrier. Current-voltage characteristics were measured up to 75 V in air to test the metallization. © 2012 American Institute of Physics. [<http://dx.doi.org/10.1063/1.4729802>]

I. INTRODUCTION

Au is commonly used in electronic device research as contact metallization, often with a thin layer of Ti to promote adhesion, with Si or Si-containing compound as the most common substrates.^{1–10} Unfortunately, Si and Au react eutectically at 363 °C, and this reaction limits the applicability of such contact to low temperatures. Devices incorporating nanowires can sometimes reach high temperatures due to a high wire resistance leading to a detrimental reaction of the contact that affects its integrity and function. Such high temperature may either be reached gradually during current-voltage (*IV*) measurement or result from a momentary pulse due to electrostatic discharge. Figure 1 shows the result of an unintentional electrostatic discharge, where a ZnO nanowire was placed on top of a 4H-SiC substrate with a semi-insulating (SI) epilayer and contacted using Ti/Au contact metallization (voltage and current unknown). The original purpose of this material choice was to create nanowire electronic device that will be stable at high temperatures. In the case shown, the nanowire was unaffected. However, the metallization reacted with the substrate and partially melted. For another example, in cases where the nanowire was GaN, Au reacted eutectically with Ga from the nanowire as well. In those cases, we observed the GaN nanowire to melt along with the metallization. In this work, we examine the introduction of a Ti-Si-N diffusion barrier between the top Au and the Ti to improve the survivability of the device. Ti-Si-N belongs to a class of ternary films of the type TM-Si-N (TM being Ti, Ta, Mo, or W). These films stand out by their excellent performance as barrier materials, preventing interdiffusion or reaction between Al, Cu, or Au and Si.¹¹ For

example, a 100-nm-thick Ti-Si-N film effectively blocks the interdiffusion between Si and Cu up to 850 °C for a 30 min annealing in vacuum.¹² These films also show oxidation resistance and have been proposed to replace the classic TiN diffusion barrier which oxidizes at temperature of 500 °C.¹³

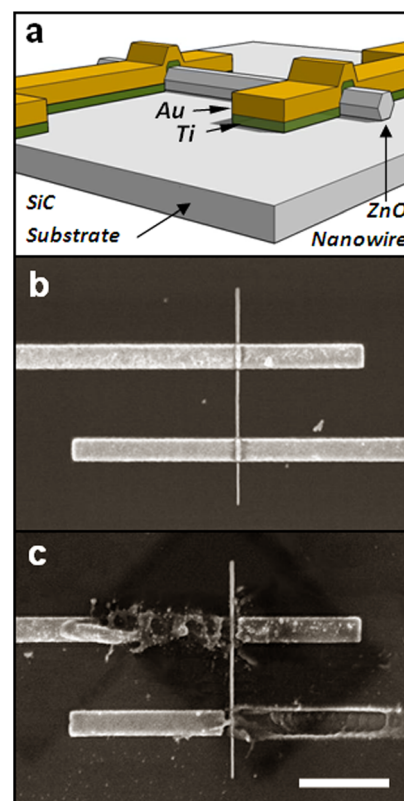


FIG. 1. ZnO nanowire device incorporating a Ti/Au metallization on a SiC substrate: (a) schematic drawing, (b) SEM image before, and (c) after an accidental electrostatic discharge. The metallization is seen to melt close to the contact with the nanowire, while the nanowire remains intact. Bar is 2 μm .

^{a)}Author to whom correspondence should be addressed. Electronic mail: shalish@ee.bgu.ac.il.

II. EXPERIMENTAL DETAILS

The 4H-SiC wafer (CREE Research, Inc.) used in this work was p-type, 280 μm thick, with a 10 μm -thick SI epilayer grown on its Si face. ZnO nanowires were grown on Si using a Au catalyst. The wires were grown by chemical vapor deposition in a tube furnace. As a source of Zn, we used a 1:1 mixture of ZnO and graphite powders. The growth was carried out at 1000 $^{\circ}\text{C}$ in a flow of 100 SCCM Ar and 0.5 SCCM O_2 . All nanowires used in this study were grown on the same growth run and were dry-transferred to the SiC substrate. Contacts were defined using lithography and lift-off. Prior to wire transfer, the samples were degreased in organic solvents in an ultrasonic bath (n-hexane, acetone, and methanol, sequentially). Immediately before the deposition, the samples were etched in an aqueous solution of 1% HF for 10 s and then blown dry with N_2 gas.

All films in this study were deposited by rf-sputtering using a planar magnetron cathode. The substrate plate was neither cooled nor heated externally. The background pressure was 4×10^{-7} Torr prior to the sputter deposition. The different layers were deposited sequentially in the same chamber without breaking vacuum. They were all deposited at 10 mTorr total pressure and 300 W rms forward sputtering power. The Ti adhesion layers and the Au overlayers were deposited in Ar discharges. The Ti-Si-N films were deposited in a discharge of Ar/ N_2 gas mixture using a Ti_5Si_3 target. The flow ratio of N_2 to Ar (0.032) and the total gas pressure (10 mTorr) were adjusted by mass flow controllers and monitored with a capacitive manometer in a feedback loop.

Three sets of SiC samples were prepared: one set of SiC/Au(210 nm), another set of SiC/Ti(20 nm)/Au(210 nm), and a third set of SiC/Ti(20 nm)/ $\text{Ti}_{29}\text{Si}_{21}\text{N}_{50}$ (100 nm)/Au(200 nm) in which a $\text{Ti}_{29}\text{Si}_{21}\text{N}_{50}$ layer was introduced as a diffusion barrier between the Ti adhesion layer and the gold overlayer. Contacts for the nanowire devices were deposited on the same deposition with the blanket deposited SiC samples and a graphite reference sample. The calculated composition of the ternary barrier layer was $\text{Ti}_{29 \pm 2}\text{Si}_{21 \pm 1}\text{N}_{50 \pm 4}$ (referred to as TiSiN in the rest of the text for brevity). It was calculated from the backscattering peak heights in the graphite reference sample.

The first two sets were annealed in vacuum of 5×10^{-7} Torr at 500 $^{\circ}\text{C}$ for 30 min. Of the third set, one sample was annealed for 30 min at 850 $^{\circ}\text{C}$ in an evacuated tube furnace (5×10^{-7} Torr), whereas the second sample was annealed at 500 $^{\circ}\text{C}$ in Ar ambient for 120 h (5 days). The heat treatment was carried out in an open-ended quartz-tube furnace. A nominally inert atmosphere was maintained by a gas flow fed directly from a cylinder of conventional-grade argon.

Before and after the thermal annealing, the samples were characterized by 2 MeV 4He^{++} backscattering spectrometry to determine compositional profiles and monitor interdiffusion or reactions in the samples.¹⁴ The thicknesses of the films were obtained from the widths of the corresponding signals in the backscattering spectra of the as-deposited films. Samples of the third set were also characterized by x-ray photoelectron spectroscopy (XPS) to determine compositional profiles and to monitor possible diffusion of light

elements such as nitrogen to which backscattering is less sensitive. XPS measurements were carried out in ultrahigh vacuum (3×10^{-10} Torr) using a PHI 5600 Multitechnique System with spherical capacitance analyzer and monochromatized Al K α radiation (1486.6 eV) source at a pass energy of 117 eV and an energy interval of 0.125 eV/step. Photoelectron spectra were acquired over a 400-mm-diameter spot. The C(1s) peak position at the surface before the sputtering at 284.8 eV was used as an energy reference.

III. RESULTS AND DISCUSSION

Figure 2(a) shows backscattering spectra of a 210 nm-thick Au film on 4H-SiC before and after 30 min annealing in vacuum at 500 $^{\circ}\text{C}$. A reaction is observed and Si is seen to diffuse into the Au layer all the way to the surface. Figure 2(b) shows backscattering spectra of a 210 nm-thick Au film on 20 nm thick Ti on 4H-SiC before and after 30 min annealing in vacuum at 500 $^{\circ}\text{C}$. Here, as well, a reaction is observed and Si is seen to diffuse into the Au layer all the way to the surface. As expected, the Ti adhesion layer cannot prevent the interdiffusion of the Si and the Au, and once they

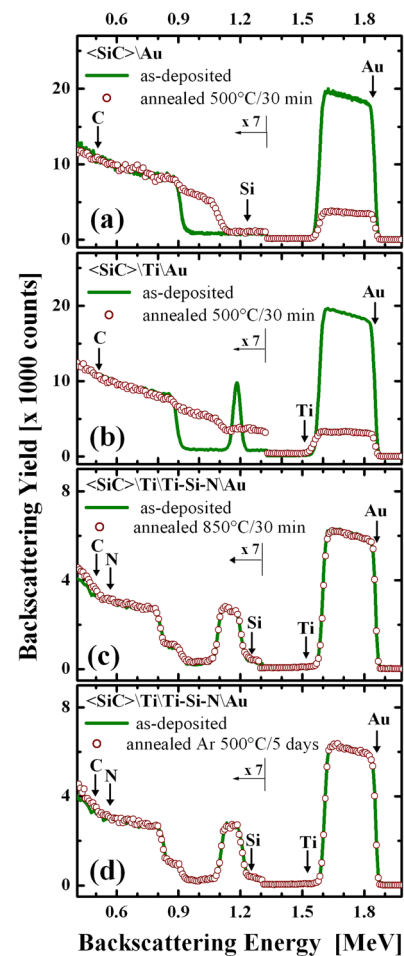


FIG. 2. Backscattering spectra of (a) 210-nm-thick Au film on 4H-SiC before and after 30 min annealing in vacuum at 500 $^{\circ}\text{C}$, (b) 210-nm-thick Au film on 20 nm thick Ti on 4H-SiC before and after 30 min annealing in vacuum at 500 $^{\circ}\text{C}$, (c) 200-nm-thick Au film on a 100 nm thick TiSiN barrier layer and 20 nm thick Ti on 4H-SiC before and after 30 min annealing in vacuum at 850 $^{\circ}\text{C}$, and (d) sample of the same sequence annealed in Ar at 500 $^{\circ}\text{C}$ for 5 days. Arrows mark the surface energies of C, N, Si, Ti, and Au.

interdiffuse, only a few percents of Si are enough to melt the Au top layer, as can be seen in Fig. 1(b). To prevent this diffusion, we used the TiSiN ternary layer. Barrier layers of similar composition were studied by Sun *et al.* for Cu metallization of Si substrates.¹¹ Layers of similar composition were also used as a barrier in similar Au metallization of AlN.¹⁵ Figures 2(c) and 2(d) show backscattering spectra of a 200 nm-thick Au film on a 100 nm thick TiSiN barrier layer and 20 nm thick Ti on 4H-SiC before and after 30 min annealing in vacuum at 850 °C, and sample of the same layer sequence annealed in Ar at 500 °C for 5 days. No change is observed in the spectra after the annealing. The Au remarkably survives both annealing treatments.

As backscattering is less sensitive to light elements, we used XPS to compare nitrogen diffusion in the sample annealed to 850 °C. Figure 3 presents XPS depth profiles of Ti(2p_{3/2}) and N(1s) as a function of the sputtering time for as deposited samples and for samples annealed at 850 °C. Diffusion of nitrogen is observed from the Ti-Si-N barrier into the Ti adhesion layer. Ti is a reactive metal, and for this property, it is believed to promote adhesion. Thermodynamically, it favors reaction with light elements, such as oxygen and nitrogen, because the heat of formation of the reaction products is very negative in these cases. Since the annealing was carried out in vacuum, the only light element available is the nitrogen incorporated in the neighboring Ti-Si-N barrier layer. This nitrogen indeed showed a limited redistribution at the interface between the two layers. This redistribution may have a minor effect on the barrier integrity near the interface, but the gettering of light elements by the Ti adhesion layer in general should increase the contact resistivity. When such metallization is annealed in air, the effect on the barrier layer may again be minor,¹³ but in that case oxygen will be gettering by the Ti adhesion layer through its open sides, where it interfaces the ambient, unless

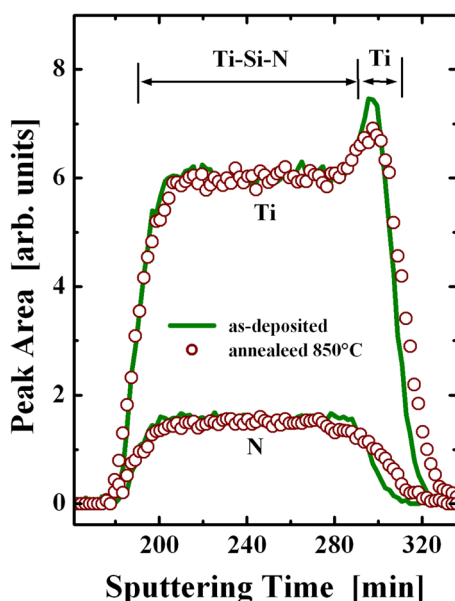


FIG. 3. X-ray photoelectron spectroscopy depth profiles of Ti(2p_{3/2}) and N(1s) in samples incorporating the Ti-Si-N barrier before and after annealing in vacuum at 850 °C, showing diffusion of nitrogen from the barrier into the Ti adhesion layer.

care is taken to block this path. The open sides render the Ti adhesion layer a vulnerable part of this metallization, and as a matter of fact, in any other metallization containing a Ti layer. Oxidation of the exposed ends of the Ti layer produces oxide that may eventually seal off the open ends impeding further oxygen diffusion.¹⁶ However, this would be gained at the cost of a loss of contact area which would typically be significant in the case of small nanowire contacts. In addition, when Ti is in contact with ZnO, as in our case, it usually reduces the ZnO, gettering its oxygen to form an interfacial Ti oxide layer.¹⁷ Both these effects are likely to increase the contact resistivity and may be evident in *IV* measurements.

To test the devices electrically, we carried out *IV* measurements in air. Figure 4 compares the current under forward bias between a device contacted with Ti/Au and a device, where a barrier layer has been employed between the Ti and the top Au. Three devices of each were tested. The results shown are typical. Reverse bias was not attempted, as the devices were electrically symmetric. The voltage was increased at a rate of 10 V/s up to 75 V and decreased back to zero at the same rate. At low voltages, the Ti/Au device shows a linear *IV* with resistance of about 12 kOhm. The resistance varied among the devices tested as each was made with a nanowire of a slightly different thickness and the carrier concentration could have fluctuated among wires of the same growth run. Between 47 and 52 V, the current is seen to drop to almost zero upon a loss of contact integrity (inset shows a SEM image of the devices after the test). On the other hand, the *IV* characteristics of the device incorporating the diffusion barrier show an initial resistance of about 15 kOhm. This device was functional all the way up to the limit of 75 V. However, its resistivity is observed to increase at high voltages and the return curve shows a higher resistance (smaller slope) of about 24 kOhm. The rate of Ti oxidation is a function of the temperature reached, the time, and the diffusion coefficient of oxygen in our sputtered-deposited Ti. The temperature is a function of the balance between the power delivered and the heat dissipated. The extreme voltage

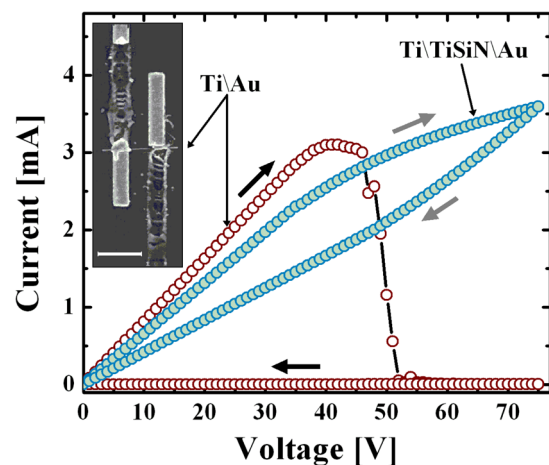


FIG. 4. Current voltage characteristics comparing a device with the Ti/Au metallization (open circles) and one incorporating a TiSiN barrier layer (filled circles). Inset shows a post-measurement image of the Ti/Au device. Bar is 2 μm .

in our test and the rate of voltage increase were meant to roughly approximate an extreme condition, such as an electrostatic discharge. Normally, such a device would be operated at less than 5 V, while an electrostatic discharge would last a fraction of a second. Under such typical conditions, the rate and the extent of oxidation should be small (note that this refers only to the diffusion barrier protected metallization. In the absence of a diffusion barrier, the metallization is typically destroyed if experiences an accidental electrostatic discharge). It is also possible to deposit an insulator,¹⁸ e.g., aluminum oxide,¹⁹ over the metallization as a barrier to reduce oxygen in-diffusion from the ambient. Nonetheless, even in the absence of such protection, the incorporation of the Ti-Si-N diffusion barrier is observed to improve the stability of the metallization by preventing the interaction of Au with Si from the substrate. The TiSiN barrier metallization survives almost twice as high power as the power at which the Ti\Au metallization breaks.

IV. CONCLUSION

Device fabrication of individual nanowires is currently still a laborious process with very small yield. Many of the fabricated devices are lost to accidental electrostatic discharges even before they are tested. The proposed metallization improves the survival of these delicate devices. The results of this study emphasize the need to consider the binary alloy phase diagrams of every pair of materials within a nanowire device, including all the constituents of the nanowire, the substrate, and the metals used, and provide proper diffusion barriers, when reactions are expected, to improve the thermal stability of nanowire devices. The studied Au metallization should be as effective on most Si containing substrates, e.g., Si, Si₃N₄, and SiO₂, and for other nanowire materials. Possible reactions of the adhesion metal and the nanowire material should be considered in each specific case, especially for high voltage or high temperature applications, and the thickness of that layer should be made as small as possible to minimize its side effect.

ACKNOWLEDGMENTS

This work was funded by a Converging Technologies Grant from the Israeli Science Foundation—VATAT.

- ¹Z.-M. Liao, Y. Lu, H.-C. Wu, Y.-Q. Bie, Y.-B. Zhou, and D.-P. Yu, "Improved performance of ZnO nanowire field-effect transistors via focused ion beam treatment," *Nanotechnology* **22**, 375201 (2011).
- ²H. A. Nilsson, P. Caroff, C. Thelander, E. Lind, O. Karlström, and L.-E. Wernersson, "Temperature dependent properties of InSb and InAs nanowire field-effect transistors," *Appl. Phys. Lett.* **96**, 153505 (2010).
- ³J. Sun, Q. Tang, A. Lu, X. Jiang, and Q. Wan, "Individual SnO₂ nanowire transistors fabricated by the gold microwire mask method," *Nanotechnology* **20**, 255202 (2009).
- ⁴S.-S. Kwon, W.-K. Hong, G. Jo, J. Maeng, T.-W. Kim, S. Song, and T. Lee, "Piezoelectric effect on the electronic transport characteristics of ZnO nanowire field-effect transistors on bent flexible substrates," *Adv. Mater.* **20**, 4557 (2008).
- ⁵V. P. Verma, H. Jeon, S. Hwang, M. Jeon, and W. Choi, "Enhanced electrical conductance of ZnO nanowire FET by nondestructive surface cleaning," *IEEE Trans. Nanotechnol.* **7**, 782 (2008).
- ⁶W.-K. Hong, D.-K. Hwang, I.-K. Park, G. Jo, S. Song, S.-J. Park, T. Lee, B.-J. Kim, and E. A. Stach, "Realization of highly reproducible ZnO nanowire field effect transistors with n-channel depletion and enhancement modes," *Appl. Phys. Lett.* **90**, 243103 (2007).
- ⁷E. N. Dattoli, Q. Wan, W. Guo, Y. Chen, X. Pan, and W. Lu, "Fully transparent thin-film transistor devices based on SnO₂ nanowires," *Nano Lett.* **7**, 2463 (2007).
- ⁸P.-C. Chang, Z. Fan, C.-J. Chien, D. Stichtenoth, C. Ronning, and J. G. Lua, "High-performance ZnO nanowire field effect transistors," *Appl. Phys. Lett.* **89**, 133113 (2006).
- ⁹J. Goldberger, D. J. Sirbuly, M. Law, and P. Yang, "ZnO nanowire transistors," *J. Phys. Chem. B* **109**, 9 (2005).
- ¹⁰F. Liu, M. Bao, K. L. Wang, C. Li, B. Lei, and C. Zhou, "One-dimensional transport of In₂O₃ nanowires," *Appl. Phys. Lett.* **86**, 213101 (2005).
- ¹¹X. Sun, J. S. Reid, E. Kolawa, and M.-A. Nicolet, "Reactively sputtered Ti-Si-N films I. Physical properties," *J. Appl. Phys.* **81**, 656 (1997).
- ¹²J. S. Reid, X. Sun, E. Kolawa, and M.-A. Nicolet, *IEEE Electron Device Lett.* **15**, 298 (1994).
- ¹³X. Z. Ding, X. T. Zeng, Y. C. Liu, and L. R. Zhao, "Effect of oxygen incorporation on structural and properties of Ti-Si-N nanocomposite coatings deposited by reactive unbalanced magnetron sputtering," *J. Vac. Sci. Technol. A* **24**, 974 (2006).
- ¹⁴For a thorough review of backscattering spectrometry, see W.-K. Chu, J. W. Mayer, and M.-A. Nicolet, *Backscattering Spectrometry* (Academic, New York, 1978).
- ¹⁵I. Shalish, S. M. Gasser, E. Kolawa, and M.-A. Nicolet, "Gold metallization for aluminum nitride," *Thin Solid Films* **289**, 166 (1996).
- ¹⁶I. Vaquila, M. C. G. Passeggi, Jr., and J. Ferrón, "Oxidation process in titanium thin films," *Phys. Rev. B* **55**, 13925 (1997).
- ¹⁷H.-K. Kim, S.-H. Han, T.-Y. Seong, and W.-K. Choib, "Electrical and structural properties of Ti\Au Ohmic contacts to n-ZnO," *J. Electrochem. Soc.* **148**, G114 (2001).
- ¹⁸S. B. Cronin, Y.-M. Lin, O. Rabin, M. R. Black, J. Y. Ying, M. S. Dresselhaus, P. L. Gai, J.-P. Minet, and J.-P. Issi, "Making electrical contacts to nanowires with a thick oxide coating," *Nanotechnology* **13**, 653 (2002).
- ¹⁹L. Gan, R. D. Gomez, C. J. Powell, R. D. McMichael, P. J. Chen, and W. F. Egelhoff, "Thin Al, Au, Cu, Ni, Fe, and Ta films as oxidation barriers for Co in air," *J. Appl. Phys.* **93**, 8731 (2003).